Journal of Hazardous Materials B129 (2006) 244–252

Journal of Hazardous Materials

www.elsevier.com/locate/jhazmat

Adsorption of Acid Blue 193 from aqueous solutions onto DEDMA-sepiolite

Adnan Özcan*, Elif Mine Öncü, A. Safa Özcan

Department of Chemistry, Faculty of Science, Anadolu University, Yunusemre Campus, 26470 Eskişehir, Turkey

Received 25 May 2005; received in revised form 24 August 2005; accepted 27 August 2005
Available online 3 October 2005

Abstract

The adsorption of Acid Blue 193 (AB193) onto dodecylethyldimethylammonium (DEDMA)-sepiolite was investigated in aqueous solution in a batch system with respect to contact time, pH and temperature. The surface modification of DEDMA-sepiolite was examined by the FT-IR technique. The pseudo-first-order, pseudo-second-order kinetic models and the intraparticle diffusion model were used to describe the kinetic data and the rate constants were evaluated. The experimental data fitted very well with the pseudo-second-order kinetic model and also followed the simple external diffusion model up to initial 10 min and then by intraparticle diffusion model up to 75 min, whereas diffusion is not only the rate-controlling step. The adsorption capacities of natural sepiolite and DEDMA-sepiolite at pH 1.5 and 20 °C were (1.19 and 2.57) × 10^{-4} mol g^{-1}, respectively. The above results indicate that DEDMA-sepiolite has around two times higher adsorption capacity than natural sepiolite. The Langmuir and Freundlich adsorption models were applied to describe the equilibrium isotherms and the isotherm constants were also determined. The Freundlich model agrees with experimental data well. The activation energy, change of Gibbs free energy, enthalpy and entropy of adsorption were also evaluated for the adsorption of AB193 onto DEDMA-sepiolite.

Keywords: Sepiolite; Adsorption; Acid dye; Surfactant; Kinetics; DEDMA-sepiolite

1. Introduction

The world-wide high level of production and use of dyes generates a large amount of colored wastewater, which gives cause for environmental concern [1]. Since a very small amount of dye in water is highly visible and may be toxic to aquatic creatures. Some toxic dyes for instance, benzidine or arlyamine based dyes are well known for their carcinogenity. Hence, the removal of color synthetic organic dyestuff from waste effluents becomes environmentally important. It is rather difficult to treat this kind of pollutants due to their synthetic origins and their mainly aromatic structure, which are biologically non-degradable. Among several chemical and physical methods such as coagulation, ultrafiltration, ozonation, oxidation, sedimentation, reverse osmosis, flotation, precipitation, adsorption process, adsorption is one of the effective techniques that have been successfully applied for color removal from wastewater due to its low maintenance costs, high efficiency and ease of operation [2–5].

Activated carbon is the most popular adsorbent for the adsorption process since it has a high surface area and thus it has a high adsorption capacity but due to difficulty and expensive of regeneration and the need of an alternative low-cost easily available adsorbent has encouraged the search for new adsorbent [6]. In this manner, natural clays for dye removal from wastewater such as sepiolite [7–10], kaolinite [11], montmorillonite [12], smectite [13] and bentonite [14,15] are being considered as alternative low-cost adsorbents. Such natural clays can be modified in a manner that significantly improves their capability to remove hydrophobic contaminants from solution. Hence, these adsorbents in this situation become organophilic since the organic functional groups of the quaternary ammonium cations are not strongly hydrated by water. These kinds of adsorbents are termed organoclays since the exchangeable inorganic cations (e.g. H^+, Na^+, Ca^{2+}) are replaced by organic cations such as quaternary ammonium compounds by ion-exchange reaction [16,17]. Hence, organoclays are powerful

* Corresponding author. Tel.: +90 222 3350580/5781; fax: +90 222 3204910.
E-mail addresses: aozcan@anadolu.edu.tr (A. Özcan), emoncu@anadolu.edu.tr (E.M. Öncü), asozcan@anadolu.edu.tr (A.S. Özcan).

0304-3894/$ – see front matter © 2005 Elsevier B.V. All rights reserved.
doi:10.1016/j.jhazmat.2005.08.037

adsorbents for a wide variety of environmental applications [18].

Most literature on dye removal is related to cationic dyes. To our knowledge, only little information exists on the use of organoclays, as an adsorbent especially sepiolite for dye removal and the data available about the removal of acid dyes onto sepiolite also needs to research [10] and the adsorption of Acid Blue 193 (AB193) onto dodecylethyldimethyl ammonium (DEDMA)-sepiolite has not been found in the literature.

Sepiolite is a fibrous hydrated magnesium silicate and a natural clay mineral with a unit cell formula $(Si_{12})(Mg_8)(O_{30})(OH)_4(OH)_2{\cdot}8H_2O$ and a general structure formed by an alternation of blocks and tunnels that grow up in the fibre direction. Each block consists of two tetrahedral silica sheets enclosing a central magnesia sheet but the silica sheets are discontinued and inversion of the silica sheets that give rise to structural tunnels. These characteristics of sepiolite make it a powerful adsorbent for organic dye molecules. In addition, some isomorphic substitutions in the tetrahedral sheets of the lattice of sepiolite, such as Al^{3+} instead of Si^{4+} form negatively adsorption sites. Such sites are occupied by exchangeable cations that compensate for the electrical charge [8,19].

The characteristics of the adsorption behavior are generally inferred in terms of both adsorption kinetics and equilibrium isotherms. The adsorption isotherms are also an important tool to understand the adsorption mechanism for the theoretical evaluation and interpretation of thermodynamic parameters [20,21].

In this study, the removal of Acid Blue 193 (AB193) from aqueous solutions using the low-cost material sepiolite as the adsorbent by batch adsorption techniques has been investigated. The common Langmuir and Freundlich equations were used to fit the equilibrium isotherm. The dynamic behavior of the adsorption was examined on the effect of initial dye concentration, temperature and pH. The adsorption rates were determined quantitatively and stimulated by the pseudo-first-order, pseudo-second-order and intraparticle diffusion kinetic models and were also tested for validity. The thermodynamic parameters also deduced from the adsorption measurements in the present study are very useful in elucidating the nature of adsorption.

2. Materials and methods

2.1. Materials

A commercial textile dye AB193 (Isolan Dark Blue 2-SGL; CI 15707) was obtained from Dystar, Turkey and used without further purification. The chemical structure of AB193 is illustrated in Fig. 1. Sepiolite was provided from Eskisehir, Turkey. It was crushed, ground, sieved through a 63 μm sieve, and dried at 110 °C in an oven for 2 h prior to use. The cation exchange capacity (CEC) and surface area determined by the methylene blue method [22] were 299.4 mmol kg^{-1} and 234.3 $m^2\,g^{-1}$, respectively.

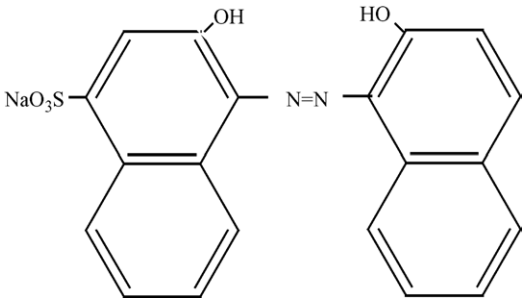

Fig. 1. Chemical structure of AB193.

2.2. Material characterization

The chemical analysis of sepiolite was determined by using an energy dispersive X-ray spectrometer (EDX-LINK ISIS 300) attached to a scanning electron microscope (SEM-Cam Scan S4). The crystalline phases present in the sepiolite were determined by using X-ray diffractometer (XRD-Rigaku Rint 2000) with Cu Kα radiation.

FT-IR spectra for sepiolite and DEDMA-sepiolite were recorded (KBr) on a Jasco FT-IR-300E Model Fourier transform infrared spectrometer to confirm the surface modification.

2.3. Preparation of DEDMA-sepiolite

The Na^+-exchanged form of clay was prepared by stirring samples for 24 h with 1 M NaCl. This was followed by several washings with deionized water and filtered to remove the excess NaCl and other exchangeable cations from the clay. The clay was then resuspended and filtered until a negative chloride test was obtained with 0.1 M $AgNO_3$.

A 20 g of the Na-saturated clay was dispensed in 0.5 dm^3 of distilled water. Dodecylethyldimethylammonium (DEDMA) bromide was used as a surfactant. DEDMA-sepiolite was prepared by adding quantities of the respective bromide salts equal to twice the cation exchange capacity of the sepiolite and stirring for 24 h. The clay was then washed with deionized water until free of salts and a negative bromide test had been obtained with 0.1 M $AgNO_3$ and it was grounded, sieved through a 63 μm sieve, and dried at 110 °C in an oven for 2 h and was used for the adsorption studies [23].

2.4. Adsorption experiments

The pH experiments were carried out by 50 ml of a 3.5×10^{-4} M dye solution with 0.05 g of natural sepiolite and DEDMA-sepiolite and the pH was carefully adjusted between 1 and 9 with adding a small amount of dilute HCl or NaOH solution using a pH meter (Fisher Accumet AB15). The dye solutions were stirred using a mechanical magnetic stirrer in a 100 ml erlenmeyer sealed flash with parafilm to avoid evaporation. The optimum pH was then determined as 1.5 and used throughout all adsorption experiments, which were conducted at various time intervals and temperatures (20, 30, 40 and 50 °C) to determine when adsorption equilibrium was reached and the maximum

removal of dye was attained. The solutions were filtered and were then subjected to quantitative analyses. The equilibrium concentrations of each solution were measured by spectrophotometer (Shimadzu UV-2101PC) at the λ_{max} value of 609 nm for AB193. The amount of the dye adsorbed onto DEDMA-sepiolite surface was determined by the difference between the initial and remaining concentration of dye solution.

The calculated adsorbed dye in equilibrium from the pseudo-first-order, pseudo-second-order kinetic models and intraparticle diffusion model used to evaluate the adsorption isotherms for the adsorption of AB193 onto DEDMA-sepiolite at constant temperatures of 20, 30, 40 and 50 °C.

3. Results and discussion

3.1. Chemical composition of sepiolite

The chemical composition of sepiolite obtained by using EDX analysis, given in Table 1, indicates the presence of silica and magnesia as major constituents along with traces of alumina, potassium, sodium, iron and titanium oxides in the form of impurities. XRD results combined with EDX analysis show that most of the magnesium is in the form of sepiolite and calcium and some of magnesium are in the form of dolomite. XRD also indicated the presence of free quartz in sepiolite. It is, thus, expected that the adsorbate species will be removed mainly by SiO_2 and MgO. The mineralogical composition of sepiolite was deduced by XRD, was 85% sepiolite, 5–10% smectite + illite, 2–3% others and 1% dolomite. Therefore, the major mineral constituent was found to be as sepiolite.

3.2. FT-IR analysis

FT-IR spectra of natural sepiolite and DEDMA-sepiolite were shown in Fig. 2. The band at 3687 cm^{-1} that corresponds to stretching (ν_{OH}) vibrations of hydroxyl groups (belong to Mg_3OH) attached to octahedral Mg ions located in the interior blocks of natural sepiolite and DEDMA-sepiolite. The band at 3622 cm^{-1} indicates that assigned to H–O–H stretching vibrations of water molecules weakly hydrogen bonded to the Si–O surface in both of samples. The broad band at 3411 cm^{-1}, observed each samples, is due to H–O–H vibrations of adsorbed water.

Table 1
The chemical composition of sepiolite

Constituents	wt.%
SiO_2	51.17
MgO	25.50
CaO	7.52
Al_2O_3	1.04
K_2O	0.80
Na_2O	0.54
Fe_2O_3	0.40
TiO_2	0.05
Loss on ignition	12.98

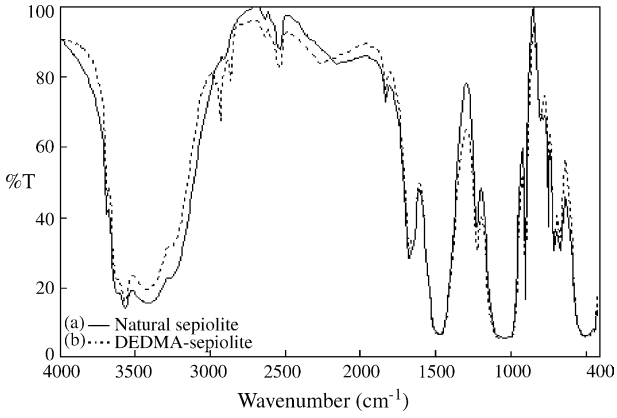

Fig. 2. FT-IR spectra of (a) natural sepiolite and (b) DEDMA-sepiolite.

A pair of strong bands at 2856 and 2929 cm^{-1} was observed only DEDMA-sepiolite can be assigned to the symmetric and asymmetric stretching vibrations of the methylene group (ν_{CH_2}) and their bending vibrations are between 1380 and 1465 cm^{-1}, supporting the intercalation of surfactant (DEDMA) molecules between the silica layers, but these stretching bands are not observed in the natural sepiolite. The band at 1664 cm^{-1} corresponds to the OH deformation of water, because the OH stretching band at 3411 cm^{-1} suggests the presence of some interlamellar water.

The Si–O coordination bands at 1211, 1033 and 881 cm^{-1} are observed as a result of the Si–O vibrations. The deep band at 1022 cm^{-1} represents the stretching of Si–O in the Si–O–Si groups of the tetrahedral sheet [24] and two peaks at 690 and 648 cm^{-1} represent the bending vibration of Mg_3OH both of samples. The bands at 530 and 471 cm^{-1} are due to Si–O–Al (octahedral) and Si–O–Si bending vibrations, respectively, for natural sepiolite and DEDMA-sepiolite.

3.3. Effect of pH

Fig. 3 indicates the effect of pH on the removal of dye (AB193) onto natural sepiolite and DEDMA-sepiolite from

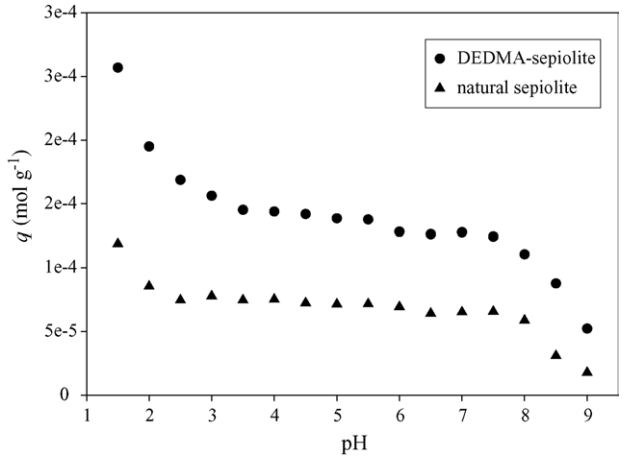

Fig. 3. Effect of pH for the adsorption of AB193 onto natural sepiolite and DEDMA-sepiolite.

aqueous solution. It was observed that the adsorption is highly dependent on pH of the solution, which affects the surface charge of the adsorbent and the degree of ionization of adsorbate. At lower pH more protons will be available, thereby increasing electrostatic attractions between negatively charged dye anions and positively charged adsorption sites and causing an increase in dye adsorption. The high adsorption capacity is due to the strong electrostatic interaction between the $–N^{+}(C_2H_5)(CH_3)_2$ of DEDMA-sepiolite and dye anions. As can be seen from Fig. 3, the maximum AB193 removal was observed at acidic pH 1.5. When the pH of the solution is increased, the positive charge on the oxide or solution interface decreases and the adsorbent surface appears negatively charged. On the contrary, a lower adsorption at higher pH values may be due to the abundance of OH^{-} ions and because of ionic repulsion between the negatively charged surface and the anionic dye molecules. There are also no exchangeable anions on the outer surface of the adsorbent at higher pH values and consequently the adsorption decreases [25].

Fig. 3 also indicates that DEDMA-sepiolite is a more effective adsorbent than natural sepiolite for adsorbing AB193. The adsorption capacity of DEDMA-sepiolite (2.57×10^{-4} mol g^{-1}) was found to be around two times higher than that of natural sepiolite (1.19×10^{-4} mol g^{-1}) at pH 1.5 and 20 °C.

3.4. Effect of initial dye concentration, contact time and temperature

The influence of the initial concentration of AB193 in the solutions on the rate of adsorption onto DEDMA-sepiolite was investigated at various concentrations at the pH value of 1.5. As shown in Fig. 4, when the initial dye concentration was increased from (2.5 to 5.0) $\times 10^{-4}$ M, the adsorption capacity of dye increased from (1.99 to 3.34) $\times 10^{-4}$ mol g^{-1}. This indicates that the initial dye concentration plays an important role in the adsorption capacities of AB193 onto DEDMA-sepiolite.

The effect of contact time on the amount of AB193, adsorbed onto DEDMA-sepiolite at 20 °C (Fig. 4) was also investigated

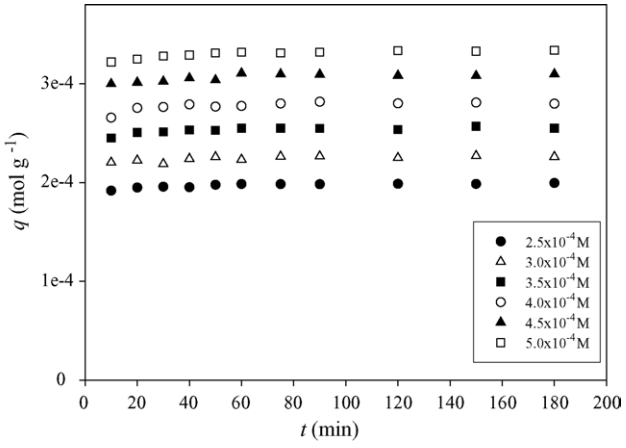

Fig. 4. Effect of initial dye concentration and contact time for the adsorption of AB193 onto DEDMA-sepiolite at 20 °C.

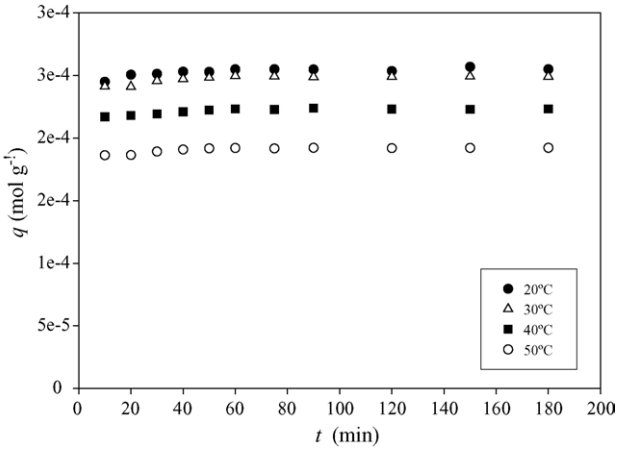

Fig. 5. Effect of temperature for the adsorption of AB193 onto DEDMA-sepiolite at the concentration of 3.5×10^{-4} M.

at the range of dye concentration 2.5–5.0 $\times 10^{-4}$ M. As can be easily seen from Fig. 4, when the equilibrium time was increased, the amount of adsorption was not increased. The rate of removal of AB193 onto DEDMA-sepiolite by adsorption was rapidly reached to equilibrium beyond which there was not significant increase in the rate of removal. Maximum adsorption of AB193 onto DEDMA-sepiolite was observed at 60 min, it can be said that beyond which there is almost no further increase in the adsorption and it is thus fixed as the equilibrium contact time.

The equilibrium adsorption capacity of AB193 onto DEDMA-sepiolite was also affected by temperature and decreased from (2.56 to 1.93) $\times 10^{-4}$ mol g^{-1} at a concentration of 3.5×10^{-4} M with increasing temperature from 20 to 50 °C (Fig. 5) (Table 2) which indicates that the adsorption of AB193 onto surfactant-modified adsorbent surface was favored at lower temperatures and it is controlled by an exothermic process. This is partly due to a weakening of the attractive forces [26,27] between AB193 and DEDMA-sepiolite. Based on the above results, it implies that physical adsorption mechanism may play a vital role in this system. Before and after equilibrium time, the adsorption capacity shows different trends at various temperatures. Below the equilibrium time, an increase in the temperature leads to an increase in dye adsorption rate, which shows a kinetically controlling process. After the equilibrium attained, the uptake decreases with increasing temperature indicating that the adsorption of AB193 onto DEDMA-sepiolite from aqueous solution is controlled by an exothermic process.

3.5. Kinetics of adsorption

Kinetics of adsorption is one of the most important characteristics to be responsible for the efficiency of adsorption. Various kinetic models such as pseudo-first-order, pseudo-second-order and intraparticle diffusion have been applied for the experimental data to predict to the adsorption kinetics. Among them pseudo-first-order rate equation is [28,29]:

$$\frac{1}{q_t} = \frac{1}{q_1} + \frac{k_1}{q_1}\left(\frac{1}{t}\right) \quad (1)$$

Table 2
Kinetic parameters and the normalized standard deviations for the adsorption of AB193 onto DEDMA-sepiolite at various temperatures

t (°C)	C_0 ($\times10^{-4}$ M)	Pseudo-first-order model				Pseudo-second-order model				Intraparticle diffusion model			
		k_1 ($\times10^{-3}$ s^{-1})	q_1 ($\times10^{-4}$ mol g^{-1})	Δq (%)	r_1^2	k_2 (dm^3 mol^{-1} s^{-1})	q_2 ($\times10^{-4}$ mol g^{-1})	Δq (%)	r_2^2	k_p ($\times10^{-7}$ mol g^{-1} s$^{-1/2}$)	C ($\times10^{-4}$ mol g^{-1})	Δq (%)	r_p^2
20	2.5	6.98	1.99	1.87	0.896	144.69	2.00	0.97	0.999	1.56	1.89	1.35	0.892
	3.0	5.22	2.26	3.20	0.512	139.47	2.27	1.91	0.999	1.37	2.17	2.71	0.551
	3.5	7.57	2.56	1.63	0.929	132.04	2.56	0.74	0.999	2.17	2.42	1.18	0.880
	4.0	9.65	2.82	1.94	0.927	126.72	2.81	1.33	0.999	2.66	2.63	1.24	0.685
	4.5	6.35	3.09	2.37	0.681	107.15	3.10	1.37	0.992	2.55	2.93	3.04	0.821
	5.0	6.67	3.34	2.31	0.915	86.88	3.35	2.31	0.999	2.37	3.17	2.63	0.907
30	3.5	7.20	2.50	2.33	0.801	166.13	2.50	1.33	0.999	2.33	2.35	0.95	0.891
40	3.5	6.06	2.24	2.25	0.824	192.48	2.24	1.23	0.999	1.65	2.13	0.90	0.941
50	3.5	6.70	1.93	3.45	0.828	213.26	1.93	1.40	0.999	1.59	1.82	1.05	0.879

where q_1 and q_t are the amounts of the dye adsorbed at equilibrium and at time t, in mol g^{-1}, and k_1 is the pseudo-first-order rate constant (s^{-1}), was applied to the present study of dye adsorption. Values of k_1 calculated from the slope of the plots of $1/q_t$ versus $1/t$ are shown in Table 2. It was found that the correlation coefficients for the pseudo-first-order model are lower than that of the pseudo-second-order model. This indicates that the adsorption of AB193 onto DEDMA-sepiolite does not follow the pseudo-first-order kinetics.

The pseudo-second-order kinetic model [30] is expressed as

$$\frac{t}{q_t} = \frac{1}{k_2 q_2^2} + \frac{1}{q_2} t \tag{2}$$

where q_2 is the maximum adsorption capacity (mol g^{-1}) for the pseudo-second-order adsorption, q_t the amount of the dye adsorbed at time t (mol g^{-1}), k_2 the equilibrium rate constant of pseudo-second-order adsorption (dm^3 mol^{-1} s^{-1}). Values of k_2 and q_2 were calculated from the plot of t/q_t against t (Fig. 6). The calculated q_2 values agree with experimental q_2 values, and also, the correlation coefficients for the pseudo-second-order kinetic plots at all the studied concentrations were above 0.992 (Table 2). These results imply that the adsorption system studied obeys to the pseudo-second-order-kinetic model. The k_1, k_2, q_1, q_2, and correlation coefficients, r_1^2 and r_2^2 of AB193 under different conditions were calculated from relevant plots and are given in Table 2. A similar phenomenon, we have been observed in the adsorption of acid dyes by acid-activated bentonite [15] and sepiolite [10].

Adsorption kinetics are generally controlled by different mechanism, of which the most limiting are the diffusion mechanisms, including the initial curved portion, attributed to rapid external diffusion or boundary layer diffusion and surface adsorption, and the linear portion, a gradual adsorption stage due to intraparticle diffusion, followed by a plateau to equilibrium where the intraparticle diffusion starts to decrease due to the low concentration in solution phase as well as fewer available adsorption sites [31].

In general, external mass transfer or external diffusion is characterized by the initial solute uptake [32,33] and can be cal-

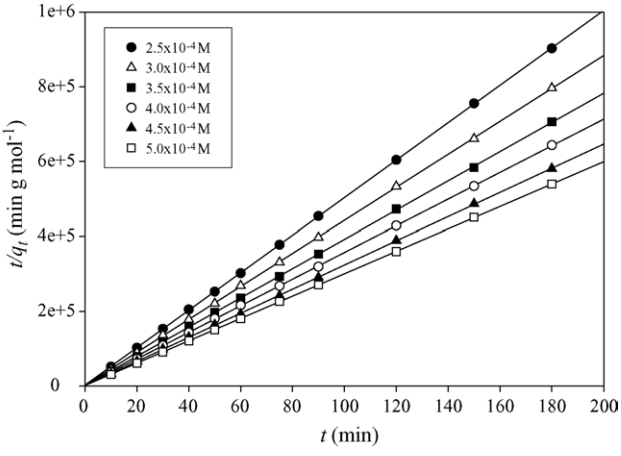

Fig. 6. Pseudo-second-order kinetic plots for the adsorption of AB193 onto DEDMA-sepiolite at 20 °C.

culated from the slope of plot of C/C_0 versus time. The slope of these plots can be calculated either by assuming polynomial relation between C/C_0 and time or it can be calculated based on the assumption that relationship was linear for the first initial rapid phase [34]. In the present study the second technique was used by assuming that the external mass transfer occurs in the first 10 min. Thus, the initial adsorption rates (mass transfer coefficient) were quantified as $(C_{10\,\mathrm{min}}/C_0)/10$. The calculated average external mass transfer coefficient value for the adsorption of AB193 onto DEDMA-sepiolite was found to be $5.07 \times 10^{-4}\,\mathrm{s}^{-1}$ at a concentration range of $2.5–5.0 \times 10^{-4}$ M at 20 °C.

The intraparticle diffusion equation [35] can be written by following:

$$q_t = k_\mathrm{p} t^{1/2} + C \tag{3}$$

where C is the intercept, and k_p is the intraparticle diffusion rate constant (mol g^{-1} $\mathrm{s}^{-1/2}$).

The pseudo-first-order and pseudo-second-order kinetic models cannot identify the diffusion mechanism and the kinetic results were then analyzed by using the intraparticle diffusion model. According to this model, the plot of uptake, q_t, versus the square root of time ($t^{1/2}$) (Fig. 7) should be linear if intraparticle diffusion is involved in the adsorption process and if these lines pass through the origin then intraparticle diffusion is the rate controlling step [36–38]. When the plots do not pass through the origin, this is indicative of some degree of boundary layer control and this further shows that the intraparticle diffusion is not the only rate-limiting step, but also other kinetic models may control the rate of adsorption, all of which may be operating simultaneously. The slope of linear portion from the figure can be used to derive values for the rate parameter, k_p, for the intraparticle diffusion, given in Table 2. The correlation coefficients (r_p^2) for the intraparticle diffusion model are between 0.551 and 0.941. This indicates that the adsorption of AB193 onto DEDMA-sepiolite may be followed by an intraparticle diffusion model up to 75 min. The values of intercept give an idea about the boundary layer thickness such the larger the intercept, the greater is the boundary layer effect.

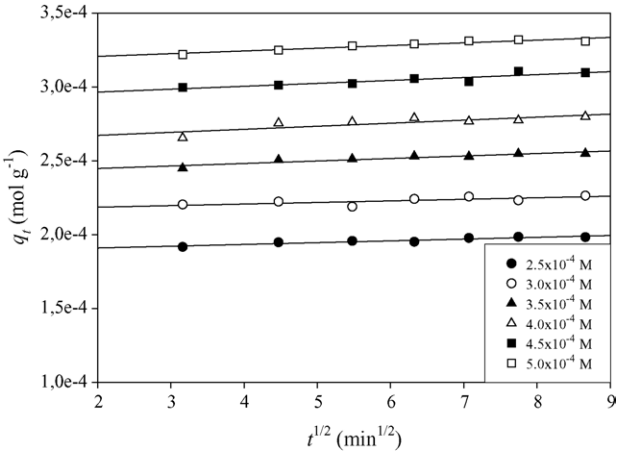

Fig. 7. Intraparticle diffusion plots for the adsorption of AB193 onto DEDMA-sepiolite at 20 °C.

As discussed above, the validity of these kinetic models can be quantitatively checked by using a normalized standard deviation Δq (%) is calculated as following equation [39]:

$$\Delta q(\%) = \sqrt{\frac{\sum [(q_\mathrm{exp} - q_\mathrm{cal})/q_\mathrm{exp}]^2}{n-1}} \times 100 \tag{4}$$

where n is the number of data points. Table 2 lists the calculated results. In the range of studied, the values of Δq for the best-fit model are less than 2.31%. It is concluded the adsorption of AB193 can be best described by the pseudo-second-order kinetic model.

The pseudo-second-order rate constants for AB193 onto DEDMA-sepiolite indicate a steady increase with temperature. The values of rate constants were found to increase from 132.04 to 213.26 $\mathrm{dm}^3\,\mathrm{mol}^{-1}\,\mathrm{s}^{-1}$ at a concentration of 3.5×10^{-4} mol dm^{-3} for DEDMA-sepiolite with an increase in the solution temperatures from 20 to 50 °C. It is confirmed that adsorption of AB193 onto DEDMA-sepiolite indicates a physisorption process. In conventional physisorption systems, increasing temperature generally increases the rate of approach to equilibrium, but decreases the equilibrium adsorption capacity [40].

3.6. Adsorption isotherms

The equilibrium adsorption isotherms are one of the most important data to understand the mechanism of the adsorption systems. Several isotherm equations are available and two important isotherms are selected in this study, which are namely the Langmuir and Freundlich isotherms.

The Langmuir adsorption isotherm assumes that adsorption takes place at specific homogeneous sites within the adsorbent and has found successful application many adsorption processes of monolayer adsorption. The linear form of the Langmuir isotherm equation is represented by the following equation [41]:

$$\frac{1}{q_\mathrm{e}} = \frac{1}{q_\mathrm{max}} + \frac{1}{q_\mathrm{max} K_\mathrm{L}} \left(\frac{1}{C_\mathrm{e}}\right) \tag{5}$$

where q_e is the equilibrium dye concentration on the adsorbent (mol g^{-1}), C_e the equilibrium dye concentration in the solution (M), q_max the monolayer adsorption capacity of the adsorbent (mol g^{-1}), and K_L is the Langmuir adsorption constant (dm^3 mol^{-1}) and related to the free energy of adsorption. A plot of $1/q_\mathrm{e}$ versus $1/C_\mathrm{e}$ for the adsorption of AB193 onto DEDMA-sepiolite (Fig. 8) gives a straight line of slope $1/(q_\mathrm{max} K_\mathrm{L})$ and intercept $1/q_\mathrm{max}$.

The Freundlich isotherm is an empirical equation employed to describe heterogeneous systems. A linear form of the Freundlich equation is [42]:

$$\ln q_\mathrm{e} = \ln K_\mathrm{F} + \frac{1}{n} \ln C_\mathrm{e} \tag{6}$$

where K_F ($\mathrm{dm}^3\,\mathrm{g}^{-1}$) and n are Freundlich adsorption isotherm constants, being indicative of the extent of the adsorption and the degree of nonlinearity between solution concentration and adsorption, respectively. The plot of $\ln q_\mathrm{e}$ versus $\ln C_\mathrm{e}$ for

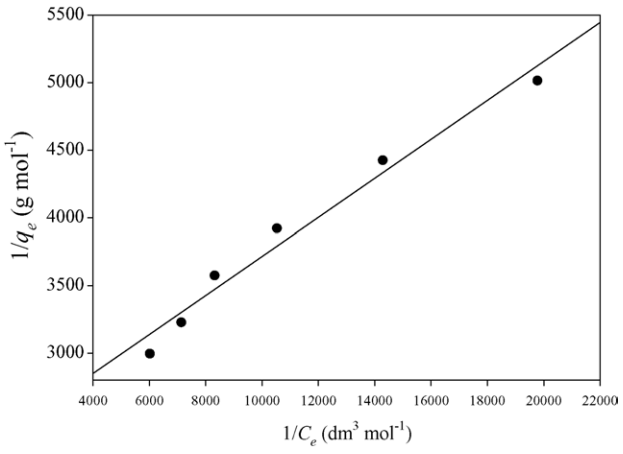

Fig. 8. Langmuir plot for the adsorption of AB193 onto DEDMA-sepiolite at 20 °C.

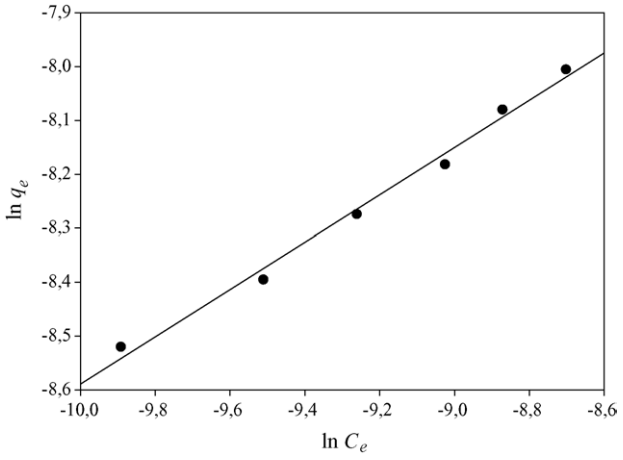

Fig. 9. Freundlich plot for the adsorption of AB193 onto DEDMA-sepiolite at 20 °C.

the adsorption of AB193 onto DEDMA-sepiolite (Fig. 9) was employed to generate the intercept value of K_F and the slope of $1/n$.

The Langmuir and Freundlich parameters for the adsorption of AB193 are listed in Table 3. It is evident from these data that the surface of DEDMA-sepiolite is made up of heterogeneous adsorption patches. In other words, Freundlich isotherm model fits very well when the r^2 values are compared (Table 3).

The effect of isotherm shape has been discussed [43] with a view to predicting whether an adsorption system is favorable or unfavorable. The essential feature of the Langmuir isotherm can be expressed by means of 'R_L', a dimensionless constant referred to as separation factor or equilibrium parameter R_L is calculated using the following equation:

$$R_L = \frac{1}{1 + K_L C_0} \tag{7}$$

where K_L is the Langmuir constant (dm^3 mol^{-1}) and C_0 is the highest initial dye concentration (M). The value of R_L calculated as above equation is incorporated in Table 3. The parameter indicates the type of isotherm to be irreversible ($R_L = 0$), favorable ($0 < R_L < 1$), linear ($R_L = 1$) or unfavorable ($R_L > 1$). This value lies between 0 and 1 [43,44], for AB193 onto DEDMA-sepiolite, the on-going adsorption process is favorable.

One of the Freundlich constants K_F indicates the adsorption capacity of the adsorbent. The other Freundlich constants n is a measure of the deviation from linearity of the adsorption. If a value for n is equal to unity the adsorption is linear. If a value for n is below to unity, this implies that adsorption process is chemical, but a value for n is above to unity, adsorption is favorable a physical process. The value of n at equilibrium is 2.277, represent favorable adsorption, and therefore this would seem to suggest that physical, which is referred the adsorption bond becomes weak [45] and conducted with van der Waals forces, rather than chemical adsorption is dominant when it is used for adsorbing AB193.

3.7. Thermodynamic parameters

Arrhenius relationship was used to evaluate the activation energy of adsorption representing the minimum energy that reactants must have for the reaction to proceed:

$$\ln k_2 = \ln A - \frac{E_a}{RT} \tag{8}$$

where E_a is the Arrhenius activation energy of adsorption, A the Arrhenius factor, R the gas constant, and is equal to 8.314 J mol^{-1} K^{-1}, and T is the solution temperature. When $\ln k_2$ is plotted against $1/T$ (Fig. 10), a straight line with slope $-E_a/R$ is obtained. The magnitude of activation energy gives a type of adsorption, which is mainly physical or chemical. The range of 5–40 kJ mol^{-1} of activation energies corresponds a physisorption mechanism or the range of 40–800 kJ mol^{-1} suggests a chemisorption mechanism [46]. The result obtained in this study is +12.55 kJ mol^{-1} indicating that the adsorption has a low potential barrier and assigned to a physisorption.

The thermodynamic parameters including change in the Gibbs free energy (ΔG°), enthalpy (ΔH°), and entropy (ΔS°),

Table 3
Langmuir and Freundlich isotherm constants for the adsorption of AB193 onto DEDMA-sepiolite at 20 °C

Langmuir				Freundlich		
q_{max} ($\times 10^{-4}$ mol g^{-1})	K_L ($\times 10^{-4}$ dm^3 mol^{-1})	R_L	r_L^2	n	K_F ($\times 10^{-2}$ dm^3 g^{-1})	r_F^2
4.40	1.58	0.113	0.974	2.277	1.51	0.990

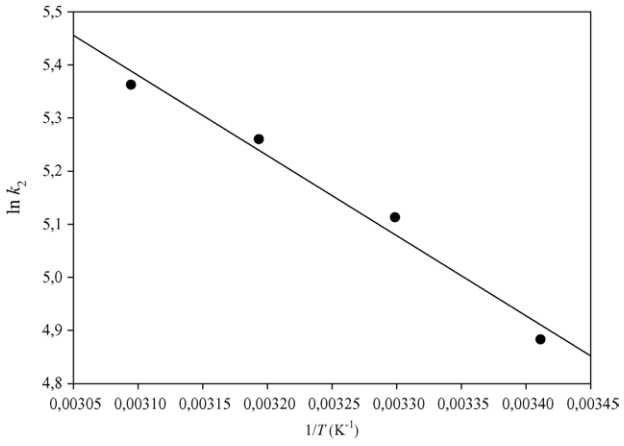

Fig. 10. Arrhenius plot for the adsorption of AB193 onto DEDMA-sepiolite.

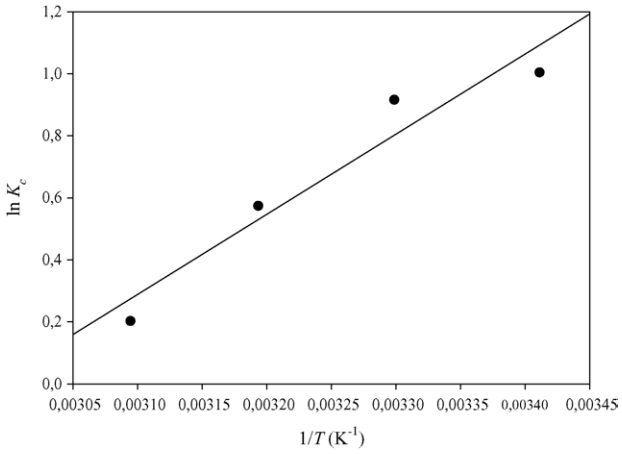

Fig. 11. Plot of ln K_C vs $1/T$ for estimation of thermodynamic parameters for the adsorption of AB193 onto DEDMA-sepiolite.

were determined by using following equations and represented in Table 4:

$$K_C = \frac{C_A}{C_S} \quad (9)$$

$$\Delta G^\circ = -RT \ln K_C \quad (10)$$

$$\ln K_C = \frac{\Delta S^\circ}{R} - \frac{\Delta H^\circ}{RT} \quad (11)$$

where K_C is the equilibrium constant, C_A the amount of dye adsorbed on the adsorbent from the solution at equilibrium (mol dm^{-3}), and C_S is the equilibrium concentration of the dye in the solution (mol dm^{-3}). The q_2 of the pseudo-second-order model in Table 2 was used to obtain C_A and C_S. ΔH° and ΔS° were calculated from the slope and intercept of van't Hoff plots of ln K_C against $1/T$ (Fig. 11). The results are given in Table 4.

Generally, the change of free energy for physisorption is between −20 and 0 kJ mol^{-1}, but chemisorption is a range of −80 to −400 kJ mol^{-1} [47]. The overall free energy change during the adsorption process was negative for the experimental range of temperatures (see Table 4), corresponding to a spontaneous physical process of AB193 adsorption and that the system does not gain energy from an external source. When the temperature decreases from 50 to 20 °C, the magnitude of free energy change shifts to high negative value (from −0.545 to −2.448 kJ mol^{-1}) suggested that the adsorption was more spontaneous at low temperature [48].

The negative value of the enthalpy change (−21.48 kJ mol^{-1}) indicates that the adsorption is physical in nature involving weak forces of attraction and is also exothermic, thereby demonstrating that the process is stable energetically [49]. The negative entropy change (ΔS°) value (−64.18 J mol^{-1} K^{-1}) corresponds to a decrease in the degree of freedom of the adsorbed species.

Table 4
Thermodynamic parameters calculated for the adsorption of AB193 onto DEDMA-sepiolite

t (°C)	E_a (kJ mol^{-1})	ΔG° (kJ mol^{-1})	ΔH° (kJ mol^{-1})	ΔS° (J mol^{-1} K^{-1})
20	12.55	−2.448	−21.48	−64.18
30		−2.310		
40		−1.495		
50		−0.545		

4. Conclusions

In this study, the equilibrium and the dynamics of the adsorption of Acid Blue 193 (AB193) onto DEDMA-sepiolite was investigated. It may be concluded that DEDMA-sepiolite can be used for elimination of textile dye effluents from wastewater. Sepiolite is a low-cost natural abundant and locally available adsorbent for dye removal and it may be alternative to more costly adsorbents such as activated carbon.

The kinetics of adsorption of AB193 onto DEDMA-sepiolite was examined by using the pseudo-first-order, pseudo-second-order and intraparticle diffusion kinetic models under different initial dye concentrations, temperatures and pHs. The pseudo-second-order and intraparticle diffusion models up to 75 min, predicts the behavior over the whole range strongly supporting the validity and agrees with physisorption being rate-controlling because it is basically based on the adsorption capacity. The obtained maximum adsorption capacity of DEDMA-sepiolite for AB193 at pH around 1.5 is due to the strong electrostatic interactions its adsorption site and dye anion.

The experimental data produced perfect fit with the Freundlich isotherm showing that the surface of the sepiolite particle was heterogeneous, non-specific and non-uniform in nature.

The activation energy of adsorption of AB193 onto DEDMA-sepiolite is found to be as +12.55 kJ mol^{-1}. The small positive value of E_a indicates a low potential barrier and confirms the nature of physical adsorption of AB193 onto DEDMA-sepiolite.

The enthalpy change (ΔH°) for the adsorption process was −21.48 kJ mol^{-1}, which did not indicate very strong chemical forces between the adsorbed dye molecules and DEDMA-sepiolite. The ΔG° values were negative therefore the adsorption was spontaneous and the negative value of ΔS° suggests a decreased randomness at the solid/solution interface and no significant changes occur in the internal structure of the adsorbent through the adsorption of AB193 onto DEDMA-sepiolite.

References

[1] H. Métivier-Pignon, C. Faur-Brasquet, P. Le Cloirec, Adsorption of dyes onto activated carbon cloths: approach of adsorption mechanisms and coupling of ACC with ultrafiltration to treat coloured wastewaters, Sep. Purif. Technol. 31 (1) (2003) 3–11.

[2] S.S. Dubey, R.K. Gupta, Removal behavior of Babool bark (*Acacia nilotica*) for submicro concentrations of Hg^{2+} from aqueous solutions: a radiotracer study, Sep. Purif. Technol. 41 (1) (2005) 21–28.

[3] M.S. Chiou, P.Y. Ho, H.Y. Li, Adsorption behavior of dye AAVN and RB4 in acid solutions on chemically cross-linked chitosan beads, J. Chin. Instit. Chem. Eng. 34 (6) (2003) 625–634.

[4] V.K. Garg, R. Gupta, A.B. Yadav, R. Kumar, Dye removal from aqueous solution by adsorption on treated sawdust, Bioresour. Technol. 89 (2) (2003) 121–124.

[5] A. Bhatnagar, A.K. Jain, A comparative adsorption study with different industrial wastes as adsorbents for the removal of cationic dyes from water, J. Colloid Interface Sci. 281 (1) (2005) 49–55.

[6] S.F. Montanher, E.A. Oliveira, M.C. Rollemberg, Removal of metal ions from aqueous solutions by sorption onto rice bran, J. Hazard. Mater. B117 (2–3) (2005) 207–211.

[7] F.L. Arbeloa, T.L. Arbeloa, I.L. Arbeloa, Spectroscopy of Rhodamine 6G adsorbed on sepiolite aqueous suspensions, J. Colloid Interface Sci. 187 (1) (1997) 105–112.

[8] G. Rytwo, D. Tropp, C. Serban, Adsorption of diquat, paraquat and methyl green on sepiolite: experimental results and model calculations, Appl. Clay Sci. 20 (6) (2002) 273–282.

[9] B. Armagan, O. Ozdemir, M. Turan, M.S. Çelik, Adsorption of negatively charged azo dyes onto surfactant-modified sepiolite, J. Environ. Eng. 129 (8) (2003) 709–715.

[10] A.S. Ozcan, S. Tetik, A. Ozcan, Adsorption of acid dyes from aqueous solutions onto sepiolite, Sep. Sci. Technol. 39 (2) (2004) 301–320.

[11] R.G. Harris, J.D. Wells, B.B. Johnson, Selective adsorption of dyes and other organic molecules to kaolinite and oxide surfaces, Colloids Surf. A: Physicochem. Eng. Aspect 180 (1–2) (2001) 131–140.

[12] C.-C. Wang, L.-C. Juang, T.-C. Hsu, C.-K. Lee, J.-F. Lee, F.-C. Huang, Adsorption of basic dyes onto montmorillonite, J. Colloid Interface Sci. 273 (1) (2004) 80–86.

[13] M. Ogawa, R. Kawai, K. Kuroda, Adsorption and aggregation of a cationic cyanine dye on smectites, J. Phys. Chem. US 100 (40) (1996) 16218–16221.

[14] A.S. Özcan, B. Erdem, A. Özcan, Adsorption of Acid Blue 193 from aqueous solutions onto Na–bentonite and DTMA–bentonite, J. Colloid Interface Sci. 280 (1) (2004) 44–54.

[15] A.S. Özcan, A. Özcan, Adsorption of acid dyes from aqueous solutions onto acid-activated bentonite, J. Colloid Interface Sci. 276 (1) (2004) 39–46.

[16] S.K. Dentel, A.I. Jamrah, D.L. Sparks, Sorption and cosorption of 1,2,4-trichlorobenzene and tannic acid by organo-clays, Water Res. 32 (12) (1998) 3689–3697.

[17] J.W. Stucki, J. Wu, H.M. Gan, P. Komadel, A. Banin, Effects of iron oxidation state and organic cations on dioctahedral smectite hydration, Clay Clay Miner. 48 (2) (2000) 290–298.

[18] Y.-H. Shen, Preparation of organobentonite using non-ionic surfactants, Chemosphere 44 (5) (2001) 989–995.

[19] R.E. Grim, Clay Mineralogy, McGraw Hill, New York, 1968.

[20] S.J. Allen, G. McKay, J.F. Porter, Adsorption isotherm models for basic dye adsorption by peat in single and binary component systems, J. Colloid Interface Sci. 280 (2) (2004) 322–333.

[21] S. Sohn, D. Kim, Modification of Langmuir isotherm in solution systems-definition and utilization of concentration dependent factor, Chemosphere 58 (1) (2005) 115–123.

[22] R.K. Taylor, Cation exchange in clays and mudrocks by methylene blue, J. Chem. Technol. Biotech. 35A (1985) 195–207.

[23] Z. Li, R.S. Bowman, Retention of inorganic oxyanions by organo-kaolinite, Water Res. 35 (16) (2001) 3771–3776.

[24] J. Madejová, FT-IR techniques in clay mineral studies, Vib. Spectrosc. 31 (1) (2003) 1–10.

[25] Z. Wu, I.-S. Ahn, C.-H. Lee, J.-H. Kim, Y.G. Shul, K. Lee, Enhancing the organic dye adsorption on porous xerogels, Colloids Surf. A: Physicochem. Eng. Aspect 240 (1–3) (2004) 157–164.

[26] W.T. Tsai, C.W. Lai, K.J. Hsien, Adsorption kinetics of herbicide paraquat from aqueous solution onto activated bleaching earth, Chemosphere 55 (6) (2004) 829–837.

[27] D. Singh, Effect of different factors on the adsorption of phosphamidon on two different types of Indian soil, Adsorpt. Sci. Technol. 16 (8) (1998) 583–594.

[28] Y.S. Ho, G. McKay, A comparison of chemisorption kinetic models applied to pollutant removal on various sorbents, Process Saf. Environ. Protect. 76 (B4) (1998) 332–340.

[29] Y.S. Ho, G. McKay, The kinetics of sorption of basic dyes from aqueous solution by sphagnum moss peat, Can. J. Chem. Eng. 76 (4) (1998) 822–827.

[30] Y.S. Ho, G. McKay, Kinetic models for the sorption of dye from aqueous solution by wood, Process Saf. Environ. Protect. 76 (B2) (1998) 183–191.

[31] E. Guibal, P. McCarrick, J.M. Tobin, Comparison of the sorption of anionic dyes on activated carbon and chitosan derivatives from dilute solutions, Sep. Sci. Technol. 38 (12–13) (2003) 3049–3073.

[32] G. McKay, S.J. Allen, I.F. McConvey, M.S. Otterburn, Transport processes in the sorption of colored ions by peat particles, J. Colloid Interface Sci. 80 (2) (1981) 323–339.

[33] G. McKay, S.J. Allen, Surface mass transfer processes using peat as an adsorbent for dyestuffs, Can. J. Chem. Eng. 58 (1980) 521–526.

[34] V. Vadivelan, K.S. Kumar, Equilibrium, kinetics, mechanism, and process design for the sorption of methylene blue onto rice husk, J. Colloid Interface Sci. 286 (1) (2005) 90–100.

[35] W.J. Weber Jr., J.C. Morriss, Kinetics of adsorption on carbon from solution, J. Sanitary Eng. Div. Am. Soc. Civ. Eng. 89 (1963) 31–60.

[36] N. Kannan, M.M. Sundaram, Kinetics and mechanism of removal of methylene blue by adsorption on various carbons—a comparative study, Dyes Pigments 51 (1) (2001) 25–40.

[37] K.G. Bhattacharyya, A. Sharma, Azadirachta indica leaf powder as an effective biosorbent for dyes: a case study with aqueous Congo Red solutions, J. Environ. Manage. 71 (3) (2004) 217–229.

[38] J.P. Chen, S. Wu, K.-H. Chong, Surface modification of a granular activated carbon by citric acid for enhancement of copper adsorption, Carbon 41 (10) (2003) 1979–1986.

[39] R.-S. Juang, F.-C. Wu, R.-L. Tseng, Characterization and use of activated carbons prepared from bagasses for liquid-phase adsorption, Colloids Surf. A: Physicochem. Eng. Aspect 201 (1–3) (2002) 191–199.

[40] Y.S. Ho, G. McKay, Sorption of dye from aqueous solution by peat, Chem. Eng. J. 70 (2) (1998) 115–124.

[41] I. Langmuir, The adsorption of gases on plane surfaces of glass, mica and platinum, J. Am. Chem. Soc. 40 (9) (1918) 1361–1403.

[42] H.M.F. Freundlich, Über die adsorption in lösungen, Z. Phys. Chem. 57 (1906) 385–470.

[43] T.W. Webi, R.K. Chakravort, Pore and solid diffusion models for fixed-bed adsorbers, J. Am. Instit. Chem. Eng. 20 (2) (1974) 228–238.

[44] K.R. Hall, L.C. Eagleton, A. Acrivos, T. Vermeulen, Pore- and solid-diffusion kinetics in fixed-bed adsorption under constant-pattern conditions, Ind. Eng. Chem. Fundam. 5 (2) (1966) 212–223.

[45] J.-Q. Jiang, C. Cooper, S. Ouki, Comparison of modified montmorillonite adsorbents. Part I. Preparation, characterization and phenol adsorption, Chemosphere 47 (7) (2002) 711–716.

[46] H. Nollet, M. Roels, P. Lutgen, P. Van der Meeren, W. Verstraete, Removal of PCBs from wastewater using fly ash, Chemosphere 53 (6) (2003) 655–665.

[47] M.J. Jaycock, G.D. Parfitt, Chemistry of Interfaces, Ellis Horwood Ltd., Onichester, 1981.

[48] B.S. Chu, B.S. Baharin, Y.B. Che Man, S.Y. Quek, Separation of vitamin E from palm fatty acid distillate using silica. I. Equilibrium of batch adsorption, J. Food Eng. 62 (1) (2004) 97–103.

[49] Y. Yu, Y.Y. Zhuang, Z.H. Wang, Adsorption of water-soluble dye onto functionalized resin, J. Colloid Interface Sci. 242 (2) (2001) 288–293.